# Nilsson diagrams for light neutron-rich nuclei with weakly-bound neutrons

Ikuko Hamamoto
*Division of Mathematical Physics, Lund Institute of Technology at the University of Lund, Lund, Sweden and The Niels Bohr Institute, Blegdamsvej 17, Copenhagen Ø, DK-2100, Denmark*
(Received 16 July 2007; published 26 November 2007)

Using Woods-Saxon potentials and the eigenphase formalism for one-particle resonances, one-particle bound and resonant levels for neutrons as a function of quadrupole deformation are presented, which are supposed to be useful for the interpretation of spectroscopic properties of some light neutron-rich nuclei with weakly bound neutrons. Compared with Nilsson diagrams in textbooks that are constructed using modified oscillator potentials, we point out a systematic change of the shell structure in connection with both weakly bound and resonant one-particle levels related to small orbital angular momenta $\ell$. Then, it is seen that weakly bound neutrons in nuclei such as $^{15-19}$C and $^{33-37}$Mg may prefer being deformed as a result of the Jahn-Teller effect, due to the near degeneracy of the $1d_{5/2}$-$2s_{1/2}$ levels and the $1f_{7/2}$-$2p_{3/2}$ levels in the spherical potential, respectively. Furthermore, the absence of some one-particle resonant levels compared with the Nilsson diagrams in textbooks is illustrated.

DOI: 10.1103/PhysRevC.76.054319 PACS number(s): 21.60.Ev, 21.10.Pc, 27.20.+n, 27.30.+t

## I. INTRODUCTION

The study of one-particle motion in spheroidal potentials, which is the basis for the understanding of deformed nuclei, started in the fifties [1–4]. In particular, the work by S. G. Nilsson [3] played an important role for years in providing the basis for the classification of experimental data on the spectra of stable odd-$A$ deformed nuclei [5]. Because the nucleon separation energy in stable nuclei is 7–10 MeV, the spectroscopic analysis around the ground state of those nuclei has been successfully performed in terms of harmonic-oscillator wave functions. In contrast, the recent study of nuclear structure close to the neutron drip line points out the unique role of weakly bound neutrons with small angular momentum $\ell$ and the importance of coupling to the nearby continuum of unbound states. Due to the absence of the Coulomb barrier, weakly bound neutrons with small $\ell$ have an appreciable probability of being outside the core nucleus. Thus, those neutrons are insensitive to the strength of the potential provided by the well-bound nucleons in the system. In particular, the behavior of $s_{1/2}$ neutrons is an extreme example because of the absence of the centrifugal barrier for the $\ell = 0$ orbit, compared with weakly-bound large $\ell$ neutrons, of which wave functions stay mostly inside the potential. The $\ell(\ell+1)$ dependence of the height of the centrifugal barrier affects sharply the presence (or absence) of one-particle resonant levels at a given positive energy. Taking spheroidal Woods-Saxon potentials, the properties of both weakly bound neutron orbits and one-neutron resonant levels are studied in Refs. [6–8].

There have been a number of self-consistent Hartree-Fock (HF) calculations of light neutron-rich nuclei, in many of which deformed HF solutions are indeed obtained. (As a classic work we refer the reader to Ref. [9].) However, almost all those calculations have been done either using the expansion in terms of harmonic oscillator bases or confining the system in a finite box. To our knowledge, no deformed HF calculation is yet available that is carried out by integrating in mesh of space coordinate with proper asymptotic behavior for $r = R_{\max}$, at which the nuclear potential is negligible. If deformed HF calculations are carried out in the latter way, the numerical results are totally independent of the values of $R_{\max}$ and, furthermore, it becomes possible to estimate one-particle resonant levels without any ambiguity.

The effective interactions to be used in HF calculations of nuclei far away from the stability line are not yet properly fixed. Thus, if the interaction chosen is not appropriate for those nuclei away from the stability line, the answer is not reliable. Moreover, one HF solution gives one self-consistent deformation, which is determined by the two-body interaction selected, assuming that all technical problems in obtaining HF solutions are solved. Thus, it is not easy either to pin down the origin of the deformation obtained or to evaluate the ambiguity coming from the choice of the two-body interaction.

In the analysis of observed spectroscopic properties of light neutron-rich nuclei with weakly bound neutrons the shell model is so far used in most cases. The shell model should be applicable to those nuclei if the configuration space is sufficiently large and the weakly bound particles are properly treated. The latter condition is usually not satisfied, because harmonic-oscillator wave functions in a limited space are used in most cases. The work summarized in Ref. [10] is an exception among the calculations that can be systematically compared with experiments; however, the complicated calculations have so far been carried out only for the helium and oxygen isotopes. In any case, some physically interesting quantities such as one-particle energies (or shell structure) or nuclear shape (or deformation) are not directly obtained from shell model calculations.

Recognizing how useful it was to have Nilsson diagrams in the study of stable deformed nuclei [5], which are constructed using modified oscillator potentials, in this article we present some "Nilsson diagrams" that are relevant especially to some light neutron-rich nuclei toward the neutron drip line. Taking the Woods-Saxon potentials with the parameters adjusted to

 

some particular nuclei, both bound and resonant one-neutron levels are calculated as a function of quadrupole deformation. The change of nuclear shell structure for neutrons is seen in both negative and positive one-particle energies of the Nilsson diagrams. The change comes from the unique behavior of neutron orbits with small $\ell$ values, in particular $\ell = 0$ and 1. The modified shell structure has direct relevance to the ground and low-lying states of neutron-drip-line nuclei, in which weakly bound neutrons are present. Considering the possible absence of many-body pair-field in light nuclei, the study of the present type of Nilsson diagrams can definitely help us to understand the origin of possible deformation and the related spectroscopic properties of light neutron-drip-line nuclei.

In Sec. II some points of our model are summarized. Numerical results are presented in Sec. III. Conclusions and discussions are given in Sec. IV.

## II. MODEL

The occupancy of weakly bound one-particle levels has a contribution especially to the tail of the self-consistent potentials. However, even for light nuclei presently considered the number of weakly bound neutron(s) is much smaller than that of well-bound core nucleons. In other words, the major part of the nuclear potential is provided by well-bound nucleons. Thus, for simplicity, the parameters of Woods-Saxon potentials are taken from the standard ones [11] for stable nuclei except for the depth, $V_{\rm WS}$. Namely, the diffuseness, the strength of spin-orbit potentials, and the radius parameter are taken from those on p. 239 of Ref. [11]. The depth is adjusted so that a particular one-neutron level obtains a given desirable binding-energy in respective examples.

The way in which bound one-particle levels are calculated is described in Ref. [6], while the eigenphase formalism that is used to estimate one-particle resonant levels for a deformed potential is given in Refs. [7,8]. The essential point is that the coupled equations obtained from the Schrödinger equation are solved in coordinate space with the correct asymptotic behavior of wave functions for $r \to \infty$. The solution obtained in this way is totally independent of the upper limit of radial integration, $R_{\rm max}$, if both the potential and the coupling term are already negligible at $r = R_{\rm max}$. One-particle resonant energy for $\beta \neq 0$ is defined as the energy at which one of the eigenphases increases through $\pi/2$ as energy increases. In the limit of $\beta \to 0$ this definition in the eigenphase formalism is in agreement with the definition of one-particle resonance in spherical potentials described in textbooks [12]; the phase shift increases through $\pi/2$ as energy increases.

One-particle resonance is not obtained if none of the calculated eigenphases do not increase through $\pi/2$ as energy increases. For example, we have no corresponding resonance in the case where a calculated eigenphase starts to decrease before reaching $\pi/2$ as energy increases. Even if one fails to obtain one-particle resonance defined in terms of eigenphase, for a certain small region of energy just after the disappearance of resonance the concentration of the wave functions inside the potential may still be found. However, the concentration will easily disappear after a short time if a resonance is no longer obtained in the eigenphase formalism. This situation is analogous to the case of the spherical potential, in which the phase shift starts to decrease before reaching $\pi/2$ as energy increases [12].

Compared with the Nilsson diagram based on modified oscillator potentials, the striking difference of the level scheme obtained in the present work comes from the behavior of levels with low $\ell$ values (in particular, $\ell = 0$ and 1) for $\beta = 0$ and those with small $\Omega$ values (mainly $\Omega^\pi = 1/2^+, 1/2^-$, and $3/2^-$) for $\beta \neq 0$, in both the weakly bound and positive-energy regions. Note that the minimum $\ell$ value of possible components of $\Omega^\pi = 1/2^+, 1/2^-$, and $3/2^-$ levels is equal to 0, 1 and 1, respectively. The absence of the centrifugal barrier for the $\ell = 0$ channel produces the unique behavior of weakly bound and positive-energy $\Omega^\pi = 1/2^+$ orbits. However, we find that some $\Omega^\pi = 1/2^+$ resonant levels survive in a higher-energy region (see, for example, the [200 1/2] level in Fig. 1) if the relative probability of the $s_{1/2}$ component inside the potential is smaller than a certain critical value [8]. Because the height of the centrifugal barrier becomes lower for a larger nuclear radius, the unique behavior of $\ell = 1$ components will be more easily seen in nuclei with larger mass.

## III. NUMERICAL RESULTS

### A. Neutron-rich C isotopes

Taking $V_{\rm WS} = -40.0$ MeV and the radius parameter for $A = 17$, at $\beta = 0$ in Fig. 1 we obtain $\varepsilon(1d_{5/2}) = -560$ keV

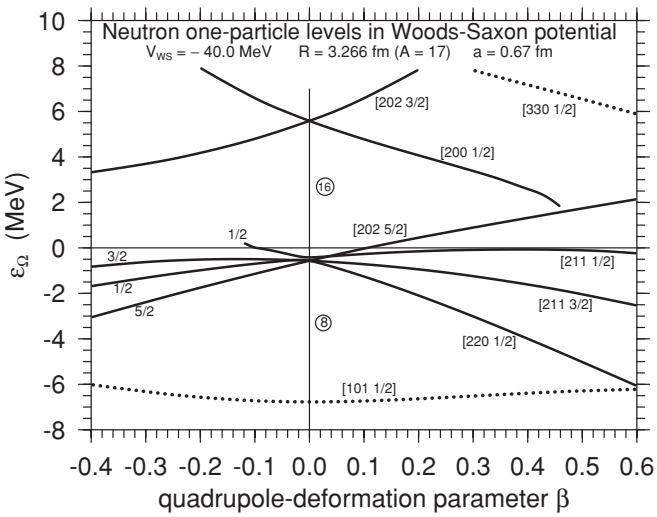


FIG. 1. Neutron one-particle levels as a function of quadrupole deformation. Parameters of the Woods-Saxon potential are designed approximately for the nucleus $^{17}$C. One-particle levels are denoted by the asymptotic quantum numbers [N $n_z \Lambda \Omega$]. The $\Omega$ values are denoted for four positive-parity levels for $\beta < 0$, because it may be difficult to see the connection to the levels for $\beta > 0$. One-particle levels appearing at $\beta = 0$ are $1p_{1/2}$, $1d_{5/2}$, $2s_{1/2}$, and $1d_{3/2}$ levels at $-6.77$, $-0.56$, $-0.42$, and $+5.60$ MeV, respectively. One-particle levels in the positive-energy region, of which the phase shift (one of the eigenphases) for $\beta = 0$ ($\beta \neq 0$) does not increase through $\pi/2$ as energy increases, are not plotted. The neutron numbers 8 and 16, which are obtained by filling in all lower-lying levels, are indicated with circles.

and $\varepsilon(2s_{1/2}) = -415$ keV. The resonant energy of the $1d_{3/2}$ level is 5.60 MeV. The near degeneracy of the $1d_{5/2}$ and $2s_{1/2}$ levels compared to the high-lying $1d_{3/2}$ level exhibits that for the spherical shape the neutron number $N = 16$ may behave like a magic number. For $\beta \neq 0$ the $s_{1/2}$, $d_{3/2}$, $d_{5/2}$, $g_{7/2}$, and $g_{9/2}$ channels are included in the calculation of positive-parity levels, while the $p_{1/2}$, $p_{3/2}$, $f_{5/2}$, and $f_{7/2}$ channels are included for negative-parity levels. The parameters are chosen approximately for neutrons in the nucleus $^{17}_{6}C_{11}$, because the observed neutron separation energy of $^{17}C$ is $-730$ keV and the nucleus is presumably prolately deformed. Examining the Nilsson diagram in Fig. 1, it is seen that a few neutrons occupying the weakly bound almost-degenerate $1d_{5/2}$-$2s_{1/2}$ shells at $\beta = 0$ may prefer being deformed to gain the total energy. This may be the case for neutrons in $^{15,17,19}C$, in which the neutron separation energy is small. It is also noticed that the observed ground states of $^{17}_{6}C_{11}$ and $^{19}_{6}C_{13}$ with $I^{\pi} = 3/2^{+}$ and $1/2^{+}$, respectively, may be in a natural way interpreted as the bandheads of the intrinsic [211 3/2] and [211 1/2] configurations for prolate deformation, when the level scheme in the Nilsson diagram is applied to those nuclei. For some experimental evidence for the deformation of those C isotopes, see, for example, Refs. [13,14].

The [220 1/2] resonant level is not obtained for $\beta < -0.12$ and $\varepsilon_{\Omega} > 0.22$ MeV, because the predominant component of the [220 1/2] wave function inside the nuclear radius is $s_{1/2}$ and thus decays very quickly [8]. Due to the same reason, the continuation of the [200 1/2] resonant level cannot be found for $\beta > 0.46$ and $0 < \varepsilon_{\Omega} < 1.82$ MeV, while for smaller $\beta$ values the predominant component of the [200 1/2] level inside the nuclear radius is $d_{3/2}$ and thus the resonant level is sufficiently well defined.

To illustrate the near degeneracy of the $2s_{1/2}$ and $1d_{5/2}$ levels at $\beta = 0$ in Fig. 1, in Fig. 2 the energy eigenvalues of Woods-Saxon potentials are shown, which were obtained by varying the depth while keeping other parameters the same as those in Fig. 1. The $2s_{1/2}$ level crosses with the $1d_{5/2}$ level for $|V_{\rm WS}|$ slightly smaller than 40 MeV. For reference, the value of $V_{\rm WS}$ that is obtained by applying Eq. (2–182) of Ref. [11] to $^{17}_{6}C_{11}$ is $-41.3$ MeV.

If a larger diffuseness, $a > 0.72$ fm, is used in Fig. 1, keeping other parameters of the Woods-Saxon potential unchanged, for $\beta = 0$ the $2s_{1/2}$ level appears lower than the $1d_{5/2}$ level. Nevertheless, in the region of an appreciable size of deformation the structure of the Nilsson diagram coming from the $2s_{1/2}$ and $1d_{5/2}$ levels remains approximately the same.

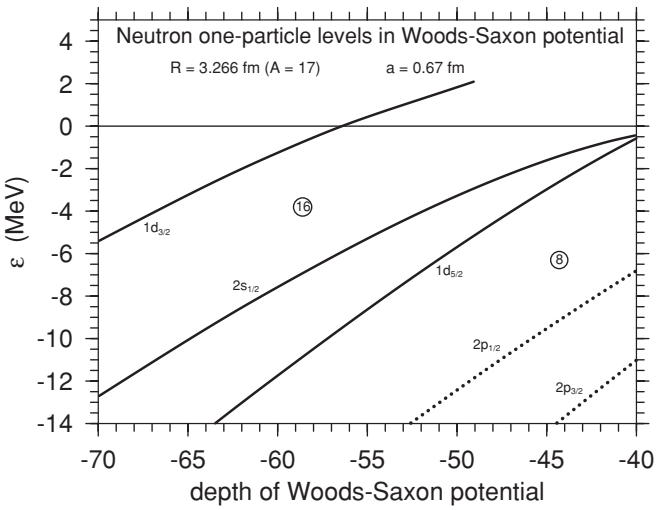


FIG. 2. Neutron one-particle levels as a function of the depth of Woods-Saxon potential, $V_{\rm WS}$, for $\beta = 0$. All parameters other than $V_{\rm WS}$ are the same as those in Fig. 1. Note that $V_{\rm WS} = -40$ MeV is used in Fig. 1. The $\ell = 2$ one-particle resonant level continues to be well defined above $\varepsilon = 2$ MeV.

### B. Neutron-rich Mg isotopes

Taking $V_{\rm WS} = -40.0$ MeV, in Fig. 3 the Nilsson diagram for neutrons is plotted for the radius appropriate for $A = 31$. For the parameters of Fig. 3 the $2s_{1/2}$ level for $\beta = 0$ is well bound and, therefore, it lies approximately in the middle of the $2d_{5/2}$ and $2d_{3/2}$ levels just as obtained from the level scheme in the modified oscillator potential [5], in contrast to the near degeneracy of the $2s_{1/2}$-$1d_{5/2}$ levels shown in Fig. 1. For $\beta \neq 0$ the $s_{1/2}$, $d_{3/2}$, $d_{5/2}$, $g_{7/2}$, and $g_{9/2}$ channels are included in the calculation of positive-parity levels, while the $p_{1/2}$, $p_{3/2}$, $f_{5/2}$, $f_{7/2}$, $h_{9/2}$, and $h_{11/2}$ channels are included for negative-parity levels. The value of $V_{\rm WS}$ is chosen so that the spin parities of the ground state of nuclei $^{31}_{12}Mg_{19}$ and $^{33}_{12}Mg_{21}$, $1/2^{+}$ [15] and $3/2^{-}$ [16], respectively, are obtained

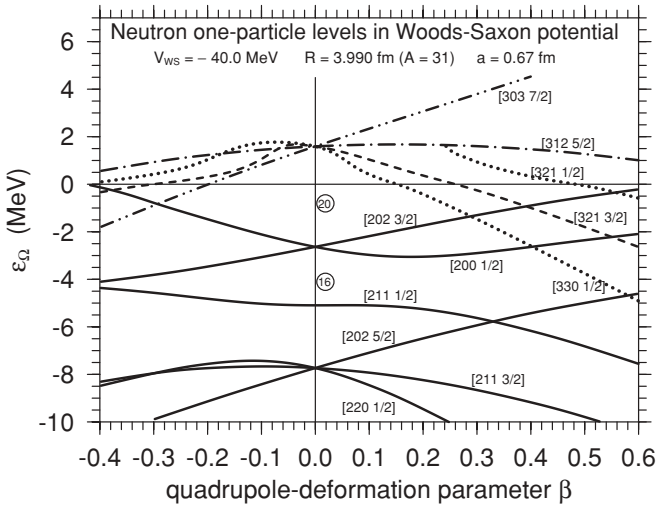


FIG. 3. Neutron one-particle levels as a function of quadrupole deformation. Parameters of the Woods-Saxon potential are designed approximately for the nucleus $^{31}Mg$. The $\Omega^{\pi} = 1/2^{-}$ levels are denoted by dotted curves, the $3/2^{-}$ levels by dashed curves, the $5/2^{-}$ levels by dot-dashed curves, and the $7/2^{-}$ levels by dot-dot-dashed curves, while positive-parity levels are plotted by solid curves. One-particle levels appearing at $\beta = 0$ are $1d_{5/2}$, $2s_{1/2}$, $1d_{3/2}$, and $1f_{7/2}$ levels, from the bottom to the top. Neither $2p_{3/2}$ nor $2p_{1/2}$ levels are obtained at $\beta = 0$ as one-particle resonant levels and, thus, they are not plotted in the figure. The next low-lying one-particle resonant level for $\beta = 0$ is the $1f_{5/2}$ level at 8.96 MeV that lies outside the range of the figure. See the text for details and also the legend to Fig. 1.

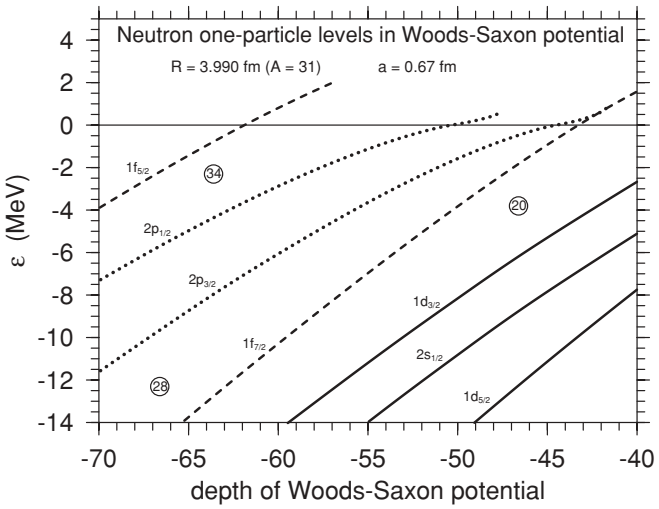


FIG. 4. Neutron one-particle levels as a function of the depth of Woods-Saxon potential, $V_{\rm WS}$, for $\beta = 0$. All parameters other than $V_{\rm WS}$ are the same as those in Fig. 3. Note that $V_{\rm WS} = -40$ MeV is used in Fig. 3. The $\ell = 3$ one-particle resonant levels continue to be well defined above $\varepsilon = 2$ MeV, while the $2p_{3/2}$ and $2p_{1/2}$ resonant levels do not survive for $\varepsilon > 0.80$ MeV and $\varepsilon > 0.62$ MeV, respectively.

for $\beta \approx 0.5$ [17–19], which may be identified as the bandheads of the [200 1/2] and [321 3/2] configurations with observed energies of about $-2$ MeV.

The $1f_{7/2}$ resonant level at $\beta = 0$ is obtained at $\varepsilon_\Omega = 1.59$ MeV. In contrast, the $2p_{3/2}$ and $2p_{1/2}$ resonant levels are not obtained, while the trace of the $2p_{3/2}$ resonant level is expected to lie below the $1f_{7/2}$ resonant level (see Fig. 4). Nevertheless, the energy is too high for the existence of a resonance with $\ell = 1$. The complicated behavior of the energies of the $\Omega^\pi = 1/2^-$ and $3/2^-$ levels for $\beta < 0$ and below 2 MeV in Fig. 3 indicates the influence of the $2p_{3/2}$ and $2p_{1/2}$ levels, which do not appear as resonant states around $\beta = 0$. More precisely speaking, if we take the $\Omega^\pi = 1/2^-$ level plotted by the dotted curve as an example, the slope in the region of $\beta < -0.3$ indicates the $2p_{3/2}$ level at $\beta = 0$ lying lower than the $1f_{7/2}$ level, while the slope for $-0.2 < \beta < -0.14$ denotes the $2p_{1/2}$ level at $\beta = 0$ lying higher than the $1f_{7/2}$ level. This illustrates the fact that the coupling of the resonant $\Omega^\pi = 1/2^-$ level with other $\Omega^\pi = 1/2^-$ levels, which are not obtained as resonant levels and thus are not plotted in Fig. 3 for $\varepsilon_\Omega > 0$, is properly taken into account in the present work, as a result of obtaining the Nilsson levels by solving the coupled differential equations.

To locate the trace of the $2p_{3/2}$ and $2p_{1/2}$ levels for $V_{\rm WS} = -40$ MeV in Fig. 3, in Fig. 4 the energy eigenvalues of Woods-Saxon potentials are shown as a function of $V_{\rm WS}$ while keeping other parameters the same as those in Fig. 3. The $2p_{3/2}$ and $2p_{1/2}$ resonant levels are not obtained for $\varepsilon > 0.80$ MeV and $\varepsilon > 0.62$ MeV, respectively, while the $\ell = 3$ one-particle resonant levels continue to be well defined above $\epsilon = 2$ MeV. From Fig. 4 it is seen that the $2p_{3/2}$ resonant level crosses with the $1f_{7/2}$ resonant level around $V_{\rm WS} = -42$ MeV. Because in the present parametrization of Woods-Saxon potential the strength of the spin-orbit potential is proportional to $V_{\rm WS}$, it is somewhat misleading to draw the figure like Fig. 4 for a large variation of $V_{\rm WS}$. Nevertheless, using Fig. 4 it is easy to locate the trace of the $2p_{3/2}$ resonant level for $V_{\rm WS} = -40$ MeV, which is the depth used in Fig. 3.

The fact that the trace of the $2p_{3/2}$ resonant level is expected to lie below the $1f_{7/2}$ level in the positive energy region of Fig. 3 indicates that $N = 28$ is not a magic number in the example. The near degeneracy of the $1f_{7/2}$ and $2p_{3/2}$ levels in the positive-energy region is indeed similar to the level scheme of almost degenerate $1d_{5/2}$ and $2s_{1/2}$ bound levels in Fig. 1. This near degeneracy gives certainly the origin of possible deformation when a few weakly bound neutrons occupy the $1f_{7/2}$-$2p_{3/2}$ shell. Namely, the degeneracy can be used to take a particular combination of the components so as to lower some level energy as deformation sets in. This situation may correspond to neutron-rich Mg isotopes.

In Fig. 3 the level coming from the $2p_{1/2}$ level is totally missing because it does not exist as a resonant level. The level denoted as [321 1/2] is obtained as a resonant level only for $\beta > 0.24$ and $\varepsilon_\Omega < 1.67$ MeV. For $\beta < 0.24$ the energy of the level becomes larger than 1.67 MeV, and the width becomes extremely large because $\ell = 1$ is the predominant component of the wave function inside the nuclear radius. Therefore, the level cannot be identified as a resonance. The one-particle resonant level obtained for $\beta = 0$, which lies next lowest to $1f_{7/2}$, is the $1f_{5/2}$ level found at 8.96 MeV that lies outside the range of Fig. 3.

Taking $V_{\rm WS} = -40.0$ MeV, in Fig. 5 the Nilsson diagram is plotted for the radius appropriate for $A = 37$. The $1f_{5/2}$ and $2p_{3/2}$ resonances at $\beta = 0$ are found at 5.22 and 0.018 MeV with the widths 2.08 and 0.005 MeV, respectively. Using $\varepsilon(1f_{7/2}) = -0.66$ MeV, the distance between the $1f_{7/2}$ and $2p_{3/2}$ levels is 680 keV, which is again very small compared with the distance obtained in the case where both levels are

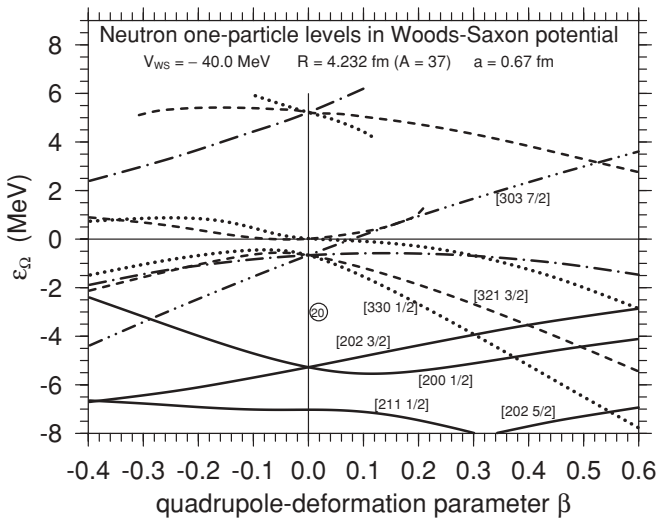


FIG. 5. Neutron one-particle levels as a function of quadrupole deformation. Parameters of the Woods-Saxon potential are designed approximately for the nucleus $^{37}$Mg. One-particle levels appearing at $\beta = 0$ are $2s_{1/2}$, $1d_{3/2}$, $1f_{7/2}$, $2p_{3/2}$, and $1f_{5/2}$ levels at $-7.02$, $-5.28$, $-0.66$, $+0.018$ and $+5.22$ MeV, respectively. The $2p_{1/2}$ level is not obtained as a one-particle resonant level. See the legend to Fig. 3 and the text for details.

well bound. This near degeneracy of the $1f_{7/2}$ and $2p_{3/2}$ levels at $\beta = 0$ suggests that weakly bound neutrons in nuclei with $N = 21$–$26$ may prefer being deformed. In the calculation of Fig. 5 for $\beta \neq 0$ the $s_{1/2}$, $d_{3/2}$, $d_{5/2}$, $g_{7/2}$, and $g_{9/2}$ channels are included in the calculation of positive-parity levels, while the $p_{1/2}$, $p_{3/2}$, $f_{5/2}$, $f_{7/2}$, $h_{9/2}$, and $h_{11/2}$ channels are included for negative-parity levels. The value of $V_{\rm WS}$ is chosen so as to simulate the nucleus $^{37}_{12}\mathrm{Mg}_{25}$, which may have a neutron separation energy of a few hundreds keV.

The $2p_{1/2}$ resonant level is not obtained at $\beta = 0$, and for $\beta \neq 0$ no $\Omega^\pi = 1/2^-$ one-particle level connected to the possible $2p_{1/2}$ level can survive as a resonant level. The $\Omega^\pi = 3/2^-$ resonant level (denoted by the dashed curve in Fig. 5) connected to the $2p_{3/2}$ level at $\beta = 0$ cannot survive for $\beta > 0.21$ and $\varepsilon_\Omega > 1.31$ MeV, because the predominant component of the wave function inside the nuclear radius is $\ell = 1$ and the level decays out quickly because of the low centrifugal barrier. The $\Omega^\pi = 1/2^-$ resonant level (denoted by the dotted curve in Fig. 5) coming from the $1f_{5/2}$ level cannot survive as a resonance for $\beta > 0.12$ because of the increasing $\ell = 1$ component inside the nuclear radius.

In the region of a few MeV excitation energy of Fig. 5, for both spherical and prolate shapes, we find no well defined one-neutron resonant levels except the [303 7/2] level, because Nilsson levels expected in the region have either $\Omega^\pi = 1/2^-$ or $3/2^-$.

It is noted that the energy distance between the $1f_{7/2}$ and $2p_{3/2}$ levels at $\beta = 0$ in the Woods-Saxon potential becomes as large as several MeV when both levels are well bound, as known from the presence of the magic number $N = 28$ in stable nuclei.

## IV. CONCLUSIONS AND DISCUSSIONS

A few examples of Nilsson diagrams with both bound and resonant levels are given, the parameters of which are chosen to be appropriate for some light neutron-rich nuclei with weakly bound neutrons, using Woods-Saxon potentials. The absence of centrifugal barrier (very low centrifugal barrier) for $\ell = 0$ ($\ell = 1$) neutrons produces the $2s_{1/2}(2p_{3/2})$ level close to the $1d_{5/2}(1f_{7/2})$ level, for both weakly bound and low-lying resonant neutrons. This near degeneracy of the $2s_{1/2}$-$1d_{5/2}$ and $2p_{3/2}$-$1f_{7/2}$ levels at $\beta = 0$ is recognized as a basic element of producing deformation for some neutron-rich C-Mg isotopes, in the case that the proton configuration allows the deformation. Here the simple argument that a larger one-particle level density around the Fermi level at the spherical point may lead to a possible deformation is based on the following known fact: In very light nuclei the many-body pair correlation may be neglected in a good approximation. If pair correlation is neglected, nuclei with a few nucleons outside a closed shell are already deformed, because using the near degeneracy of one-particle levels those nucleons have a possibility of gaining energy by breaking spherical symmetry (the Jahn-Teller effect). To quantify this statement on the deformation of weakly bound nuclei, the deformed HF calculations with an appropriate two-body interaction have to be performed, taking properly into account the weakly bound and positive-energy nucleons without expanding the wave functions in terms of harmonic-oscillator wave functions and without restricting the system in a small finite box.

One-neutron resonant levels for $\beta \neq 0$ are estimated using the eigenphase formalism. The $\Omega^\pi = 1/2^+$ resonant level can hardly survive when the predominant component of the wave function inside the potential is $s_{1/2}$, while the $\Omega^\pi = 1/2^-$ and $3/2^-$ resonant levels are not obtained if the predominant component has $\ell = 1$ and the energy is higher than 2 MeV in nuclei with $A > 16$. Nevertheless, the coupling of the bound (or resonant) $\Omega^\pi$ level with other $\Omega^\pi$ levels, which are not obtained as resonant levels, is properly taken into account in the present work, because we obtain the Nilsson levels by solving coupled differential equations. In some nuclei the absence of those $\Omega^\pi = 1/2^+$, $1/2^-$, and $3/2^-$ resonant levels produces a low density of one-neutron resonant levels in the region of several MeV. How much the low density affects the many-body correlation such as pair correlation in nuclei toward the neutron drip line is a future problem to be studied and may be properly studied only when the many-body correlation is studied treating the nearby continuum in a reasonable manner without discretizing the spectra. However, the absence (or presence) of those one-particle resonant levels may be checked by experiments such as one-nucleon resonant scattering and one-nucleon transfer reactions. It is noted that the neutron one-particle levels obtained from Nilsson diagrams for $\beta \neq 0$ are those to be recognized as bandhead configurations of odd-$N$ nuclei. Thus, rotational states, which are constructed based on those bandhead states, should be in principle observed using a proper experimental method and those high-spin states will have narrow widths if they appear in the low-energy region.

If one fails to treat properly weakly bound neutrons or low-energy neutron resonant levels with small $\ell$, the HF $2p_{3/2}(2s_{1/2})$ level will not come down close to the $1f_{7/2}(1d_{5/2})$ level. In any case, if the $1f_{7/2}$ or $1d_{5/2}$ level is appreciably isolated, in the absence of pair correlation it may be possible to obtain an oblate shape as the deformation of the system with a few neutrons in the $1f_{7/2}$ or $1d_{5/2}$ shell. This is because a preferred deformation is oblate at the beginning of the shell filling if a single $j$ shell is isolated (for example, see Refs. [20,21]), while it is prolate if shells with different $j$ values are nearly degenerate as in the harmonic-oscillator potential [22]. It is an interesting question whether any oblate shape is observed around the ground state of light neutron-drip-line nuclei of C-Mg isotopes.

A systematic change of the shell structure in the spherical potential discussed in the present article is strictly related to the characteristic feature of the weakly bound and resonant one-particle orbits with small $\ell$ values. On the other hand, in some recent literature [23] related to the shell model the change of the shell structure of neutrons (protons) as the proton (neutron) number varies is discussed, considering the tensor force between protons and neutrons using harmonic-oscillator wave functions. Though some of the shell structure change discussed in Ref. [23] looks formally similar to that studied in the present article, the mechanism of the change of the shell structure is quite different.

[1] D. L. Hill and J. A. Wheeler, Phys. Rev. **89**, 1102 (1953).
[2] S. A. Moszkowski, Phys. Rev. **99**, 803 (1955).
[3] S. G. Nilsson, Mat. Fys. Medd. Dan. Vid. Selsk. **29**, No. 16 (1955).
[4] K. Gottfried, Phys. Rev. **103**, 1017 (1956).
[5] A. Bohr and B. R. Mottelson, *Nuclear Structure* (Benjamin, Reading, MA, 1975), Vol. II.
[6] I. Hamamoto, Phys. Rev. C **69**, 041306(R) (2004).
[7] I. Hamamoto, Phys. Rev. C **72**, 024301 (2005).
[8] I. Hamamoto, Phys. Rev. C **73**, 064308 (2006).
[9] X. Campi, H. Flocard, A. K. Kerman, and S. Koonin, Nucl. Phys. **A251**, 193 (1975).
[10] A. Volya and V. Zelevinsky, Phys. Rev. C **74**, 064314 (2006).
[11] A. Bohr and B. R. Mottelson, *Nuclear Structure* (Benjamin, Reading, MA, 1969), Vol. I.
[12] For example, see R. G. Newton, *Scattering Theory of Waves and Particles* (McGraw-Hill, New York, 1966).
[13] Z. Elekes *et al*., Phys. Lett. **B586**, 34 (2004).
[14] Z. Elekes *et al*., Phys. Lett. **B614**, 174 (2005).
[15] G. Neyens *et al*., Phys. Rev. Lett. **94**, 022501 (2005).
[16] D. T. Yordanov *et al*., Phys. Rev. Lett. **99**, 212501 (2007).
[17] T. Motobayashi *et al*., Phys. Lett. **B346**, 9 (1995).
[18] H. Iwasaki *et al*., Phys. Lett. **B522**, 227 (2001).
[19] Z. Elekes *et al*., Phys. Rev. C **73**, 044314 (2006).
[20] B. R. Mottelson, in *Proceedings of the International School of Physics "Enrico Fermi" XV, 1960,* edited by G. Racah, p. 44.
[21] I. Hamamoto, B. Mottelson, H. Xie, and X. Z. Zhang, Z. Phys. D **21**, 163 (1991).
[22] A. Bohr and B. R. Mottelson, Mat. Fys. Medd. Dan. Vid. Selsk. **27**, No. 16 (1953).
[23] For example, see T. Otsuka, T. Suzuki, R. Fujimoto, H. Grawe, and Y. Akaishi, Phys. Rev. Lett. **95**, 232502 (2005).